Double Proton Transfer and One-Electron Oxidation Behaviors in Double H-Bonded Glycinamide−Formamidine Complex and Comparison with Biological Base Pair

Ping Li,[†,‡] Yuxiang Bu,*[,†,‡,§] Hongqi Ai,[†] Shihai Yan,[†] and Keli Han[§]

Institute of Theoretical Chemistry, Shandong University, Jinan 250100, People's Republic of China, Department of Chemistry, Qufu Normal University, Qufu 273165, People's Republic of China, and State Key Laboratory of Molecular Reaction Dynamics, Dalian Institute of Chemical Physics, Science Academy of China, Dalian, 116023, People's Republic of China

Received: June 5, 2004; In Final Form: August 19, 2004

The behaviors of double proton transfer (DPT) occurring in a representative glycinamide−formamidine complex have been investigated employing the B3LYP/6-311++G** level of theory. Computational results suggest that the participation of a formamidine molecule favors the proceeding of the proton transfer (PT) for glycinamide compared with that without mediator-assisted case. The DPT process proceeds with a concerted mechanism rather than a stepwise one since no zwitterionic complexes have been located during the DPT process. The barrier heights are 14.4 and 3.9 kcal/mol for the forward and reverse directions, respectively. However, both of them have been reduced by 3.1 and 2.9 kcal/mol to 11.3 and 1.0 kcal/mol with further inclusion of zero-point vibrational energy (ZPVE) corrections, where the lower reverse barrier height implies that the reverse reaction should proceed easily at any temperature of biological importance. Additionally, the one-electron oxidation process for the double H-bonded glycinamide−formamidine complex has also been investigated. The oxidated product is characterized by a distonic radical cation due to the fact that one-electron oxidation takes place on glycinamide fragment and a proton has been transferred from glycinamide to formamidine fragment spontaneously. As a result, the vertical and adiabatic ionization potentials for the neutral double H-bonded complex have been determined to be about 8.46 and 7.73 eV, respectively, where both of them have been reduced by about 0.79 and 0.87 eV relative to those of isolated glycinamide due to the formation of the intermolecular H-bond with formamidine. Finally, the differences between model system and adenine−thymine base pair have been discussed briefly.

1. Introduction

As one of the simplest and the most fundamental phenomena in the tautomeric equilibria and redox reactions, intra- or intermolecular proton transfers (PTs) play an important role in many chemical and biochemical processes.[1−3] A large number of theoretical and experimental studies have been carried out to enrich the information regarding the possible mechanisms of PTs, tautomeric equilibria, and relevant properties associated with PT processes.[1−48] Relatively, multiproton transfer phenomena, in which more than one proton is transferred with a concerted or stepwise mechanism, have not been studied extensively as the reactions of single proton transfer though they play an important role in the proton relay occurring in enzymatic reactions, transport phenomena in biological membrane, and DNA mutations.

In our previous studies,[49a,b] double proton transfer (DPT) behaviors occurring between glycinamide (or imidoformamide) and two model compounds, formamide and formic acid, have been investigated at the B3LYP/6-311++G** level of theory to get some useful information about the nature of the mechanism in multiproton-transfer processes. In those studies, the protons are transferred through a concerted mechanism and the ZPVE corrections play a key role in determining the proceeding of the reverse reactions, that is, the reverse barrier height disappears when ZPVE corrections are considered, where the disappearances of the reverse barrier height have also been reproduced by full geometry optimizations at the MP2(FULL) level and single-point energy calculations at higher-level calculations including MP3, MP4(SDQ), and CCSD(T,FULL) levels.[49a] Similar to formamide and formic acid, formamidine (or 2-aminoacetamide) is another most extensively studied system of biological importance both experimentally and theoretically. More importantly, the double H-bonded complex formed between glycinamide and formamidine possesses a similar H-bonding pattern to that in the adenine−thymine (A−T) DNA base pair. We hope that the results obtained for this relatively small model system could give some helpful implication about the possible mechanism of the PT in the A−T base pair. Thus, in the present paper, formamidine has been employed to form a double H-bonded complex with glycinamide aimed to further investigate the DPT phenomenon biologically. Additionally, one-electron oxidation behavior for the double H-bonded glycinamide−formamidine complex has also been explored since the key chemical quantity, ionization potential (IP), not only is fundamental in assessing the electron donating and accepting ability but also plays a key role in electron-transfer process occurring in the gas phase or in the condensed phase.[50,51] Expectedly, one-electron oxidation in this model system may provide some useful information to better understand the phenomenon of DNA damage caused by ionizing radiation at a molecular level, assuming that the model system can produce similar results to those of the A−T radical cation reported previously.

As one of the important components in glycinamide ribonucleotide synthetase, the relevant investigations of glycinamide

* Corresponding author. E-mail: byx@sdu.edu.cn.
† Shandong University.
‡ Qufu Normal University.
§ Science Academy of China.

10.1021/jp047567c CCC: $27.50
Published on Web 10/01/2004

have been reported theoretically and experimentally.[52−57] For example, the formations of the peptide bond in glycinamide uncatalyzed or catalyzed by the metal cations or ammonia had been extensively studied.[52−54] The unimolecular chemistry of protonated glycinamide and its proton affinity determined by mass spectrometric experiments and theoretical model were reported by Kinser et al.[55] Recently, multiply sodiated ions were observed by electronspraying glycinamide and their N-acetylated and O-amidated derivatives in the presence of sodium hydroxide, in which some sodiated glycinamide conformers were obtained at the B3LYP/6-311++G** level of theory.[56] The conformational behaviors,[57a,57b] acid−base behaviors,[57c] ionization potentials and electron affinities,[57d] and PT assisted with water molecules[57e] have been systematically investigated by us at the B3LYP/6-311++G** level of theory, where the calculated proton affinity for the global minimum, 216.81 kcal/mol, is well consistent with the experimental value of 217.23 kcal/mol.[55] In those studies,[57] the reliability of the B3LYP/6-311++G** level of theory in calculating the equilibrium geometries, frequencies, and transition states (TSs) have been verified through comparisons with the experimental data available and the higher-level calculations including MP2, MP3, MP4(SDQ), and CCSD(T) levels.

2. Computational Details

As mentioned above, all the calculations have been carried out at the B3LYP/6-311++G** level of theory since its reliability has been verified in our previous studies.[49,57]

From the global minimum of glycinamide as a starting point,[57a] the selected geometries have been fully optimized without any symmetry constraints, where glycinamide and formamidine interact with each other by means of a pair of two parallel intermolecular H-bonds as displayed in Figure 1 since what most concerns us is the DPT occurring between them. Here, three geometries associated with the DPT are denoted as **G−FI**, **TS**, and **G′−FI′** for the sake of simplicity. Normal-mode analyses have been performed to verify that the stable complexes have all positive frequencies and the transition state has only one imaginary frequency with the corresponding eigenvector pointing toward the reactants and products. To estimate the effect of ZPVE corrections on the calculated potential energy curve along the reaction coordinates, the frequencies of the nonstationary points along the intrinsic reaction coordinate (IRC) have been projected out and all other modes are constrained to be orthogonal to the gradient vector. Furthermore, the intrinsic reaction coordinate (IRC)[58] calculations in the mass-weighted internal coordinates with a step size of 0.1 amu$^{1/2}$ bohr have also been performed to further confirm the validity of the TSs. Here, the direction of the DPT from **G−FI** to **G′−FI′** is defined as the forward reaction and the reverse one is the reaction in the opposite direction.

Qualitatively, for the classical forward and reverse rate constants k^{TST}, they can be calculated through the conventional transition-state theory (TST):[4,59,60]

$$k^{TST} = \frac{k_B T}{h} \frac{Q^*}{Q^R} e^{-\Delta E_0^*/(k_B T)} \quad (1)$$

where k_B and h are the Boltzmann and Planck constants, Q^* and Q^R are the equilibrium partition functions for the TS and reactant, and ΔE_0^* is the barrier height corrected with zero-point vibrational energy (ZPVE). Additionally, the quantum

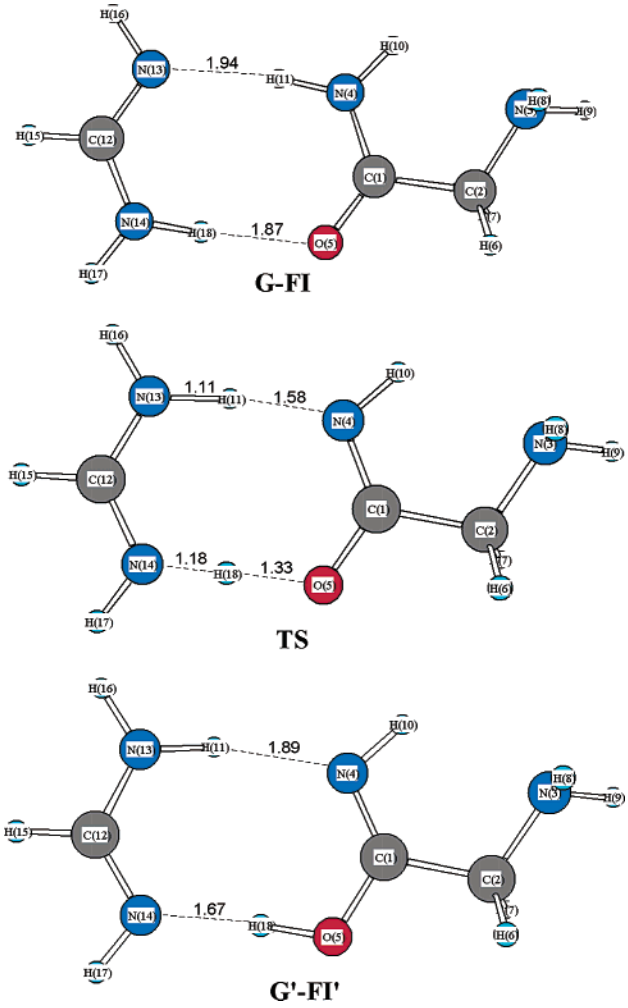

Figure 1. Optimized complex of glycinamide with formamidine and its tautomeric product together with the transition state connecting them.

mechanical tunneling effect is approximately taken into account through a tunneling transmission coefficient κ:[59,61]

$$\kappa = 1 + \frac{1}{24}\left(\frac{h\nu^*}{k_B T}\right)^2 \left(1 + \frac{k_B T}{\Delta E_0^*}\right) \quad (2)$$

where ν^* is the imaginary frequency at the TS. Thus, including the tunneling effect, the final rate constant k is given by

$$k = \kappa k^{TST} \quad (3)$$

Qualitatively, to investigate how the presence of solvent molecules affects the relevant quantities associated with the DPT processes, the isodensity surface-polarized continuum model (IPCM) within the framework of the SCRF theory,[62,63] which has been successful in the descriptions of many chemical systems in solution,[64−66] has been employed on the basis of the optimized gas-phase structures employing a series of solutions, such as chloroform, dichloroethane, acetone, nitromethane, and water (the dielectric constants ϵ = 4.9, 10.36, 20.7, 38.2, and 78.39, respectively).

In the case of ionization potential (IP), it can be obtained according to those formulas as mentioned previously.[57d] In brief, the vertical ionization potential (VIP) corresponds to the energy difference between the cationic state in the geometry of neutral state and the optimized neutral state. Certainly, the adiabatic ionization potential (AIP) corresponds to the energy difference between the optimized cationic state and the neutral state plus

TABLE 1: Selected Geometrical Parameters for Complexes of G−FI, TS, G′−FI′, and G−FI* Together with Their Dipole Moments and Rotational Constants Obtained at the B3LYP/6-311++G Level of Theory[a]**

parameter	G−FI	TS	G′−FI′	G−FI*
R(1,2)	1.53	1.53	1.52	1.97
R(1,4)	1.34	1.30	1.28	1.27
R(1,5)	1.24	1.29	1.32	1.21
R(2,3)	1.47	1.47	1.46	1.35
R(4,10)	1.01	1.02	1.02	1.01
R(4,11)	1.03	1.58	1.89	1.83
R(5,18)	1.87	1.33	1.02	1.87
R(11,13)	1.94	1.11	1.03	1.05
R(12,13)	1.29	1.32	1.34	1.31
R(12,14)	1.35	1.31	1.29	1.31
R(14,17)	1.00	1.01	1.01	1.01
R(14,18)	1.03	1.18	1.67	1.03
A(2,1,4)	116.1	121.4	124.6	115.0
A(2,1,5)	119.1	113.9	111.2	105.0
A(4,1,5)	124.8	124.7	124.2	140.1
A(1,4,11)	120.8	121.5	124.4	110.9
A(1,5,18)	122.1	117.6	113.2	115.1
A(4,11,13)	172.1	173.2	167.1	173.2
A(13,12,14)	123.4	123.1	122.9	125.0
A(11,13,12)	120.9	119.7	119.4	123.3
A(12,14,18)	120.9	122.2	124.6	122.6
D(4,1,2,3)	13.2	12.0	10.3	0.0
D(5,1,2,3)	−167.8	−168.7	−170.2	−180.0
D(2,1,4,11)	178.0	178.3	178.5	180.0
D(5,1,4,10)	−178.5	−178.3	−178.8	180.0
D(5,1,4,11)	−1.0	−0.9	−0.9	−0.0
D(2,1,5,18)	−178.1	−177.2	−177.9	−180.0
D(4,1,5,18)	0.9	2.1	1.6	0.1
D(1,4,11,13)	0.5	−0.4	−0.9	−0.4
D(1,5,14,12)	0.2	−0.1	−1.3	−0.1
D(4,11,13,12)	−0.2	0.3	0.5	0.3
D(14,12,13,11)	0.7	0.3	0.5	0.0
A[b]	4.55 (0.68)	4.62 (−2.87)	4.57 (−0.22)	4.61 (1.43)
B	0.81 (0.71)	0.91 (1.11)	0.84 (1.14)	0.77 (2.22)
C	0.69 (0.25)	0.77 (0.41)	0.72 (0.32)	0.67 (0.01)
dipole moments	1.01	3.10	1.20	2.64

[a] Bond lengths (*R*) are given in angstroms; bond angles (*A*) and dihedral angles (*D*) are given in degrees. [b] Dipole moments are given in debyes and rotational constants are given in gigahertz. The data in parentheses refer to the dipole moments along the principal axes.

thermodynamic corrections including ZPVE, vibrational, rotational, and translational corrections.

To evaluate the basis-set superposition errors (BSSEs) produced in the calculations of the interaction energies between two fragments, the Boys−Bernardi counterpoise technique has been employed.[67]

All of the computations were performed at 298.15 K and 1.0 atm by use of the Gaussian 98 program throughout.[68]

3. Results and Discussions

3.1. Double Proton-Transfer Behaviors. *3.1.1. Structural Features.* Table 1 lists selected geometrical parameters for the complexes of **G−FI**, **TS**, **G′−FI′**, and those of ionized **G−FI** (denoted as **G−FI***) together with their rotational constants and dipole moments.

As displayed in Figure 1, the selected complexes associated with the DPT are characterized by an eight-membered ring formed through a pair of two parallel intermolecular H-bonds, where all of the eight atoms of the ring are almost coplanar. As a result, both the N4−H11 and N14−H18 bonds in **G−FI** have been elongated by about 0.02 Å relative to those corresponding N4−H10 and N14−H17 bonds due to the existence of the H-bonds. Further comparisons of the H-bond contact distances and intermolecular distances between proton donors and acceptors indicate that the strengths of H-bonds formed in **G−FI** may be weaker than those formed in **G′−FI′**, implying a stronger interaction between glycinamidic acid and formamidine as discussed below. Especially, the H-bond formed between N14 and H18 should play a key role in determining the stability of **G′−FI′**. Qualitatively, this point can be understood since the donating and accepting ability of the proton donor O5 (352.0 kcal/mol) and acceptor N14 (226.3 kcal/mol) in **G′−FI′** has been increased relative to those of N14 (370.4 kcal/mol) and O5 (209.5 kcal/mol) in **G−FI**, where the data in parentheses refer to their corresponding proton affinities (PAs) obtained at the B3LYP/6-311++G** level of theory. Additionally, as an important finding in our previous studies,[57e] the corresponding barrier heights are correlated with the extent to which the angle *A*(O5C1N4) is bent, that is, the larger the degree of the compression (or expansion) of the *A*(O5C1N4), the higher the barrier height. Here, the changes of angle *A*(O5C1N4) for **G−FI** and **G′−FI′** relative to **TS** are −0.12° and 0.5°, respectively. This observation can be comparable to those findings of the PTs assisted with two-water, formamide, and formic acid molecules.[49a,b,57e] In those studies, the changes of *A*(O5C1N4) are 0.14° (1.15°), −0.62° (0.43°), and −0.61° (0.41°) relative to their corresponding transition states, where the data in parentheses refer to those relative values for tautomeric products. Analogous to the lower barrier heights in those DPT processes mentioned above,[49a,b,57e] the barrier heights for **G−FI ↔ G′−FI′** tautomeric process should be similar to them.

As far as two fragments in **G−FI** are concerned, some geometrical changes take place mainly in the regions of the intermolecular H-bonds as expected. Like those phenomena occurring in the double H-bonded complexes of glycinamide with formamide and formic acid,[49a,b] the double-bond and single-bond characteristics of the peptide bond C1−N4 and the C1−O5 bond have been strengthened, which can be reflected from their different increments in the bond lengths of −0.02 and +0.02 Å relative to those values in the isolated state.[57a] As expected, the opposite trends can be true for that of glycinamidic acid fragment in **G′−FI′** compared with its optimized isolated species. Further inspections of the dihedral angles suggest that the main skeleton angle *D*(4,1,2,3) has no significant changes (∼0.6°) and the planarity of the peptide bond has still been kept for them. On the other hand, the nonplanarity of the amino group in formamidine has been changed to be almost planar due to the existence of the intermolecular H-bonds. Overall, the geometrical changes for two fragments in **G′−FI′** are larger than those in **G−FI**, due partly to the existence of the stronger intermolecular H-bonds in the former.

Additionally, the selected geometrical changes associated with the DPT process versus reaction coordinates are displayed in Figure 2. Intuitively, the concerted mechanism of DPT in nature can be reflected qualitatively from the changes of two transferring protons, H11 and H18, along the reaction coordinates. We hope that the different changes of the distances between proton donors and acceptors, i.e., N13−N4 and N14−O5, may be helpful in understanding the dynamics of the DPT reactions.[69]

3.1.2. Interaction Energies. Table 2 summarizes the calculated interaction energies produced in the DPT process, where the interaction energy is defined as the energy difference between the optimized complexes and the sums of the optimized monomers including the ZPVE and BSSE corrections.

As displayed in Figure 1, two fragments in each complex interact with each other through a pair of two parallel intermolecular H-bonds. Comparisons of the interaction energies before and after DPT suggest that the interaction between two fragments in **G′−FI′** is larger than that of interaction in **G−FI**, where the interaction energies are −16.9 (−15.1) and −13.1 (−11.1) kcal/mol before (after) ZPVE and BSSE corrections

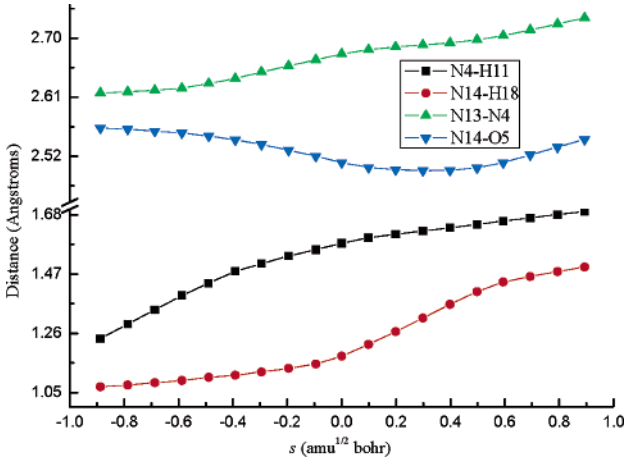

Figure 2. Selected geometrical parameter changes versus reaction coordinates *s* in the DPT process.

TABLE 2: Calculated Interaction Energies, Deformation Energies, BSSE, and ZPVE Corrections for the Interactions of Glycinamide (Glycinamidic Acid) with Formamidine[a]

	G−FI	**G′−FI′**
ΔE_{inter} [b]	−13.1 (−11.6) [−11.1]	−16.9 (−15.7) [−15.1]
ΔE_{ZPVE}	1.5	1.2
ΔE_{BSSE}	0.5	0.6
ΔE_{defor} [c]	0.8 (0.7)	2.9 (1.1)

[a] All the units are in kilocalories per mole. [b] The data in parentheses and brackets refer to those with ZPVE and further BSSE corrections, respectively. [c] The data in parentheses refer to those of the formamidine fragment.

for the former and the latter, respectively. This point is also consistent with the above conclusions drawn only from the comparison of the intermolecular H-bond contact distances since the strengths of the intermolecular H-bonds can be reflected from the calculated interaction energies qualitatively. Additionally, as listed in Table 2, further inclusions of ZPVE and BSSE corrections lower the interaction energies by about 1.9 kcal/mol, relatively smaller than those produced in multiwater-assisted PTs.[57e]

Presumably, the deformation energy can be used to assess the degrees of structural changes or interaction between two fragments upon complexation, where the deformation energy is defined as the energy difference between the neutral states at the geometries in the complexes and their corresponding optimized isolated states qualitatively. As listed in Table 2, the larger deformation energies for the fragments of glycinamidic acid (2.9 kcal/mol) and formamidine (1.1 kcal/mol) in **G′−FI′** relative to those of glycinamide (0.8 kcal/mol) and formamidine (0.7 kcal/mol) in **G−FI** give an additional evidence for the existence of the stronger intermolecular H-bonds in the former than in the latter. Even so, as described below, the double-proton-transferred product **G′−FI′** is still higher in energy by about 10 kcal/mol than **G−FI** since the favorable stability gained from the intermolecular H-bond for the former is too small to predominate over the intrinsic instability of the isolated glycinamidic acid relative to glycinamide.

3.1.3. Barrier Heights. Preliminary to understanding the mechanism of the DPT, we have constructed the potential energy surface (PES) of **G−FI** through scanning its N4−H11 and N14−H18 bonds simultaneously without optimizing the remaining parameters. Qualitatively, there are three stationary points on the PES, corresponding to two minima separated by a saddle point (**TS**). Actually, those zwitterionic structures resulting from the stepwise mechanism have collapsed to **G−FI** during the full geometry optimizations. Thus, the stepwise mechanism for the DPT has been excluded. Additionally, as displayed in Figure 2, analyses of the geometrical changes versus reaction coordinates and the eigenvector of the imaginary frequency in **TS** also suggest that the DPT mechanism should be considered as a concerted and mostly asynchronous one.

TABLE 3: Calculated Tautomeric Energies Δ*E*, ZPVE Corrections, and Barrier Heights Δ*E for the Forward and Reverse Reactions in the PT Processes[a]**

	Δ*E* [Δ*H*]	Δ*E**$_f$	Δ*E**$_r$
B3LYP	10.5 (10.3) [10. 1]	14.4 (11.3)	3.9 (1.0)
ΔE_{ZPVE}	−0.2	−3.1	−2.9

[a] All the units are in kilocalories per mole. The data in parentheses refer to those considering ZPVE corrections. Forward and reverse reactions are noted by f and r subscripts, respectively.

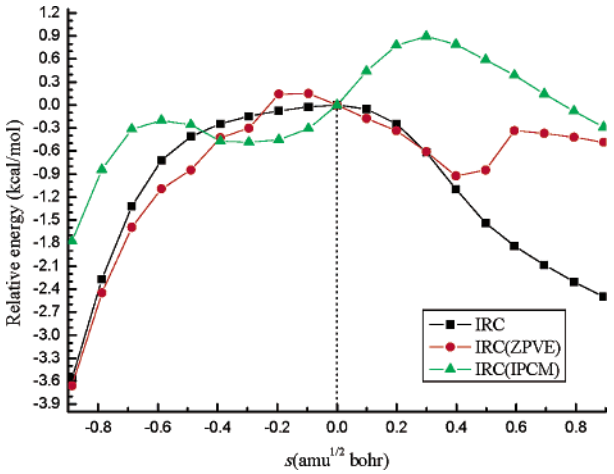

Figure 3. Calculated potential energy curves relative to the energy of the point at $s = 0.0$ amu$^{1/2}$ bohr along the reaction coordinates in the DPT process.

As listed in Table 3, the forward and reverse barrier heights are 14.4 and 3.9 kcal/mol, respectively. Moreover, both of them have been reduced by about 3.1 and 2.9 kcal/mol, to 11.3 and 1.0 kcal/mol, if further ZPVE corrections are included. Here, the lower reverse barrier height implies that the reverse process should take place easily at any temperature of biological importance. Compared with that of direct intramolecular PT in glycinamide, the barrier heights in **G−FI** have been reduced significantly, where the forward and reverse barrier heights for the intramolecular PT in the isolated glycinamide are 45.4 and 30.9 kcal/mol at the B3LYP/6-311++G** level of theory. Here, the lower reverse barrier height is also well consistent with the slight changes for *A*(N4C1O5) from **G′−FI′** to **TS** as mentioned above.

As displayed in Figure 3, one might expect that the tunneling effects might be small considering the flat PES along the reaction coordinates. Approximately, the quantum mechanical tunneling effect is concluded through a tunneling transmission coefficient as mentioned above, where the calculated coefficients are only 1.21 and 1.09 s^{-1} for the forward and reverse reactions, respectively. Thus, the calculated rate constants including tunneling effects are 3.54×10^3 and 2.58×10^{11} for the forward and reverse reactions, respectively, which is required to be further confirmed by the relevant experiments if possible.

Qualitatively, the solvent effects on the barrier heights have been evaluated by employing the IPCM model on the basis of the optimized gas-phase geometries. As displayed in Figure 4, the existence of bulk solvent has only a slight influence on the barrier heights, where the largest changes in aqueous solution

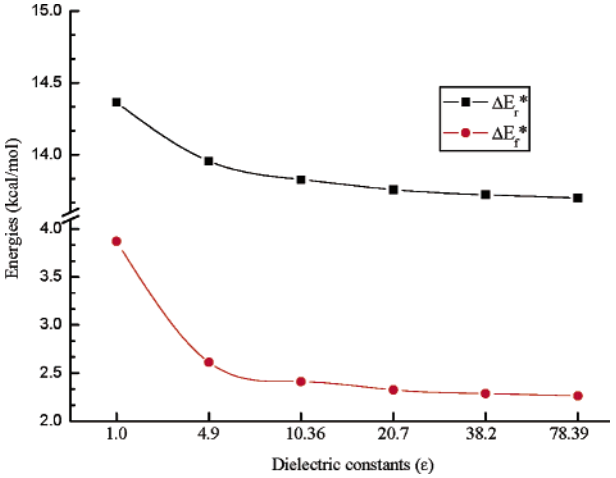

Figure 4. Dependence of the forward and reverse barrier heights on various dielectric constants in the DPT process.

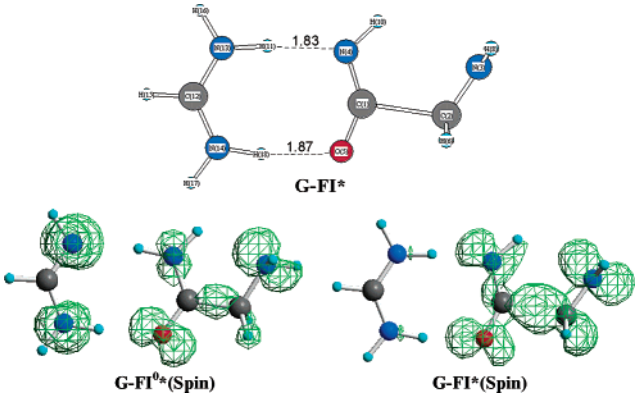

Figure 5. Optimized ionized **G−FI** and diagrams of spin density distributions for selected complexes at the B3LYP/6-311++G** level of theory, where the result of **G−FI⁰*(spin)** refers to that of cationic state at the geometry of **G−FI**.

are about −0.7 and −1.6 kcal/mol for the forward and reverse reactions compared with those in the gas phase. As expected, both barrier heights decrease with increasing dielectric constants, which is well correlated with the fact that the **TS** has a larger dipole moment (3.10 D) relative to **G−FI** (1.01 D) and **G′−FI′** (1.20 D). However, further inspections of the reverse barrier heights in various solutions ranging from 2.3 to 2.6 kcal/mol suggest that those TSs will be lower in energy than the products by about 0.3∼0.6 kcal/mol if the ZPVE corrections are considered in the gas phase (−2.9 kcal/mol). Probably, this phenomenon may be attributed to the fact that the gas-phase structures cannot serve as a reference structure for the solvent calculations as suggested by one reviewer. In view of the lack of consideration for short-range interaction with adjacent explicit solvent molecules (such as water molecules) in the IPCM model adopted here, besides a more sophisticated model for estimating the solvent effects, the geometry relaxation effects in response to the influence of the solvent molecules need to be considered in particular.

Furthermore, the ZPVE corrections and solvent effects on the calculated PES have also been investigated preliminarily due to the existence of the very flat regions around the transition state (-0.4 amu$^{1/2}$ bohr $< s < -0.1$ amu$^{1/2}$ bohr) as displayed in Figure 3. As expected, the ZPVE corrections have a significant impact on the position of the transition state, where the position of it ($s = 0.0$ amu$^{1/2}$ bohr) has been shifted to that at $s = -0.1$ amu$^{1/2}$ bohr nearby. Additionally, in analogy to a similar DPT reaction,[70] a local minimum also appears at about $s = -0.3$ amu$^{1/2}$ bohr in aqueous solution, implying that the solvent effects are strong enough to create a local minimum for this reaction, assuming that the IPCM model adopted here is suitable for the simulation of the gas-phase structure. This point can be understood since those regions are characterized by zwitterionic structures in nature.

3.1.4. Tautomeric Energy. Like that tautomerism assisted with a formic acid molecule,[49b] the tautomeric energy from **G−FI** to **G′−FI′** is 10.5 and 10.3 kcal/mol before and after consideration of ZPVE corrections as listed in Table 3, indicating the stability of **G−FI** relative to **G′−FI′**. This point can be further reflected from the calculated potential energy curve versus reaction coordinates *s* as depicted in Figure 3 qualitatively. Obviously, ZPVE corrections have a little influence on the tautomerism, though inclusion of them slightly reduces the tautomeric energy. Here, the smaller tautomeric energy relative to that of glycinamide (14.4 kcal/mol)[57e] suggests that introduction of a formamidine molecule favors the tautomeric process from glycinamide to glycinamidic acid thermodynamically.

As shown in Table 3, the relatively small values for entropy changes ΔS [about 2.4 cal/(mol·K) in absolute value] show that the Gibbs free energy changes ΔG should be essentially governed by the enthalpy changes ΔH (10.1 kcal/mol) in the tautomeric process. According to the Boltzmann statistics, i.e., $K_p = \exp(-\Delta G^\circ/RT)$, the calculated equilibrium constant is 1.23×10^{-8} at 298.15 K and 1.0 atm, which is almost equal to that of the formic acid-assisted case and much larger than those of the direct, water-, and formamide-assisted cases ranging from 1.51×10^{-15} to 5.99×10^{-10}.[49a,b,57e]

3.2. One-Electron Oxidation Process. *3.2.1. Structural Features.* On the basis of the optimized **G−FI**, we have investigated its one-electron oxidation behavior through fully optimizing its ionized geometry without any symmetry constraints. As displayed in Figure 5, similar to the neutral **G−FI**, oxidated product **G−FI*** is also characterized by a pair of two parallel intermolecular H-bonds except that the proton H11 initially attached to amide N4 in glycinamide has been transferred to N13 of formamidine, implying that the oxidation of neutral **G−FI** complex can lead to a spontaneous PT. Like that of ionized glycinamide,[57d] the interatomic distance between C1 and C2 atoms has been significantly elongated by about 0.44 Å relative to that of neutral **G−FI**, implying that the one-electron oxidation should occur on glycinamide fragment. Probably, two moieties separated by C1 and C2 atoms in glycinamide fragment and the protonated formamidine fragment should be easily observed experimentally. As a result, **G−FI*** can be regarded as a complex formed between protonated formamidine and deprotonated ionized glycinamide. Further analyses of the H-bond formed between N4 and N13 atoms suggest that oxidated product (**G−FI***) possesses a stronger H-bond relative to that before PT of H11 since it has a shorter H-bond distance and larger H-bond angle, where the H-bond distance (angle) has been shortened (increased) by about 0.11 Å (1.16°). Similarly, the elongation of N13−H11 (0.04 Å) relative to N13−H16 is also derived from the existence of this H-bond. Qualitatively, this phenomenon may be attributed to the increased basicity of glycinamide fragment resulting from the oxidation accompanying a PT to formamidine as mentioned below. Additionally, the double-bond characteristics of the peptide bond C1−N4 and the C1−O5 bond in **G−FI*** have been strengthened, which can be illustrated from the decrements in bond lengths of C1−N4

(0.07 Å) and C1−O5 (0.03 Å) relative to **G−FI**. The main skeleton angle [*D*(4,1,2,3)] in glycinamide fragment has turned out to be almost planar from that of 13.2° in **G−FI**. Moreover, as presented in Table 1, the planarity of the peptide bond in **G−FI*** has still been kept as that of neutral form.

Compared with the one-electron oxidation products of the double H-bonded complexes of glycinamide with formamide and formic acid molecules,[49a,b] **G−FI*** assumes a different structure since the other two complexes have only a single H-bond versus a double H-bond in **G−FI***. To further investigate whether there are other stable stationary points on the PES of the ionized **G−FI** or not, we have also investigated the PES of **G−FI*** through scanning its N13−H11 and N14−H18 bonds and found that there is only one stationary point on the PES, corresponding to the optimized **G−FI***. Actually, the initial designed double proton and single proton (H18) transferred structures have collapsed to **G−FI*** during the full geometry optimizations.

3.2.2. Adiabatic and Vertical Ionization Potentials. As for the neutral state of **G−FI** upon ionization, the single electron distributes evenly over the entire molecular framework before the relaxation of the system as displayed in Figure 5 [**G−FI^{0}*-(spin)**]. Furthermore, the single electron is localized mainly on the glycinamide fragment after relaxation, suggesting that ionization should take place on glycinamide. In more detail, the spin density on glycinamide fragment accounts for almost 98% of the totals. This point can be easily understood since the AIP (VIP) of formamidine 9.08 (9.51) eV is larger than that of glycinamide 8.60 (9.25) eV obtained at the B3LYP/6-311++G** level of theory. Interestingly, further inspections of the charge distributions suggest that most of the positive charges (94%) distribute over the protonated formamidine fragment, implying the nature of the single proton transfer of H11. Thus, the ionized **G−FI** should be a distonic radical cation since the charges and radical sites are separated on the different fragments. As a result, the calculated VIP and AIP of the **G−FI** are 8.46 and 7.73 eV, closer to those of glycinamide since the ionization is mainly localized on it. Compared with those of isolated glycinamide, the reductions of 0.79 and 0.87 eV for the VIP and AIP of **G−FI** should be attributed to formation of the intermolecular H-bonds with formamidine. Here, the difference of 0.73 eV between the VIP and AIP may be due to the larger geometrical differences between the ionized and neutral states as mentioned above.

4. Comparisons with A−T Base Pair

As mentioned above, the model system of **G−FI** adopted here has a similar H-binding pattern to that of A−T base pair. A question may arise, that is, how does the model system work compared with the A−T base pair? To answer this question, the selected studies of Florián et al.[18a] and Bertran et al.[11a] have been cited for comparison. As for the DPT behavior occurring between neutral A−T base pairs,[18a] studies have suggested that the origin of the stability of the A−T component of genetic code may be attributed to the very small energy barrier for the DPT together with larger energy needed for separation of the tautomeric product and the nonexistence of the zwitterionic structures during the DPT process, where the energy barriers of 9.73 and 0.22 kcal/mol for the forward and reverse reactions are well comparable to the values of 11.3 and 1.0 kcal/mol here. Obviously, the findings of Florián et al. are well reproduced by the present studies, suggesting that **G−FI** is a good model to mimic the DPT behavior of a neutral A−T base pair.

On the contrary, some apparent differences between the model system of **G−FI*** and the A−T radical cation should be mentioned.[11a] First, the ionization takes place on the adenine fragment (corresponding to formamidine) since it has a lower IP (7.38 eV) than that of thymine (8.03 eV).[71] Second, the ionization of A−T cannot lead to a spontaneous PT and the non-proton-transferred structure of A−T radical cation is still the global minimum though the single proton transferred complex (from adenine to thymine fragment) is only about 1.2 kcal/mol higher in energy and the nature of the distonic radical cation for it has also been determined. Thus, the behavior of A−T radical cation cannot be well simulated by the model system of **G−FI** though it works well for modeling the DPT process in the neutral A−T base pair.

5. Conclusions

In the present paper, the DPT process occurring between glycinamide and formamidine has been systematically investigated by employing the B3LYP/6-311++G** level of theory. The principal conclusions from this study are as follows:

1. Like those tautomeric processes directly assisted with water and formic acid molecules,[49b,57e] the participation of a formamidine molecule favors the tautomeric process for glycinamide compared with its direct tautomeric case, where the tautomeric energy from **G−FI** to **G′−FI′** is reduced by 4.1 kcal/mol thermodynamically. For the DPT process from **G−FI** to **G′−FI′**, it should proceed with a concerted mechanism rather than a stepwise one since no zwitterionic complexes have been located during the PT process. On the other hand, one-electron oxidation leads to a spontaneous PT from glycinamide to formamidine fragment, resulting in the formation of a distonic radical cation since the charges and the radical sites have been localized on the different fragments.

2. With the assistance of a formamidine molecule, the barrier heights have been reduced significantly relative to those of direct tautomerization between glycinamide and glycinamidic acid. Namely, the barrier heights in the forward and reverse directions are 14.4 (11.3) and 3.9 (1.0) kcal/mol before (after) consideration of ZPVE corrections, respectively. Here, the lower reverse barrier height implies that the reverse reaction should proceed easily at any temperature of biological importance.

3. The VIP and AIP of the neutral complex **G−FI** have been determined to be 8.46 and 7.73 eV, where the ionization is mainly localized on glycinamide fragment. Here, the difference of 0.73 eV between the AIP and VIP may be due to the larger geometrical differences between the ionized and neutral states as mentioned above.

4. The model system of **G−FI** works well for modeling the DPT behavior occurring in the neutral A−T base pair but less well for A−T radical cation.

Acknowledgment. This work was supported by the National Natural Science Foundation of China (20273040) and the Natural Science Foundation of Shandong Province (Key Project), and support from SRFDP and the Foundation for University Key Teacher by the Ministry of Education of China is also acknowledged. We are also grateful to the reviewers for their insightful suggestions to improve the presentation of the results.

References and Notes

(1) Desiraju, R. G. *Acc. Chem. Res.* **1991**, *24*, 290.
(2) Hibbert, F. *Adv. Phys. Org. Chem.* **1986**, *22*, 113.
(3) Beeman, R. W.; Matsumura, F. *Nature* **1973**, *242*, 274.
(4) Zhang, K.; Chung-Phillips, A. *J. Chem. Inf. Comput. Sci.* **1999**, *39*, 382.
(5) (a) Gorb, L.; Leszczynski, J. *Int. J. Quantum Chem.* **1998**, *70*, 855. (b) Venkateswarlu, D.; Leszczynski, J. *J. Phys. Chem. A* **1998**, *102*, 6161. (c) Gorb, L.; Leszczynski, J. *J. Am. Chem. Soc.* **1998**, *120*, 5024. (d) Gu,

J.; Leszczynski, J. *J. Phys. Chem. A* **1999**, *103*, 577. (e) Gu, J.; Leszczynski, J. *J. Phys. Chem. A* **1999**, *103*, 2744. (f) Zhanpeisov, N. U.; Cox, W. W., Jr.; Leszczynski, J. *J. Phys. Chem. A* **1999**, *103*, 4564. (g) Shukla, M. K.; Leszczynski, J. *J. Phys. Chem. A* **2000**, *104*, 3021. (h) Podolyan, Y.; Gorb, L.; Leszczynski, J. *J. Phys. Chem. A* **2002**, *106*, 12103. (i) Gorb, L.; Podolyan, Y.; Leszczynski, J.; Siebrand, W.; Fernández-Ramos, A.; Smedarchina, Z. *Biopolymers* **2002**, *61*, 77. (j) Zhanpeisov, N. U.; Leszczynski, J. *J. Phys. Chem. A* **1999**, *103*, 8317. (k) Leszczynski, J. *J. Phys. Chem. A* **1998**, *102*, 2357.

(6) Wang, X.; Nichols, J.; Feyereisen, M.; Gutowski, M.; Boatz, J.; Haymet, A. D. J.; Simons, J. *J. Phys. Chem.* **1991**, *95*, 10419.

(7) (a) Bell, R. L.; Taveras, D. L.; Truong, T. N.; Simons, J. *Int. J. Quantum Chem.* **1997**, *63*, 861. (b) Bell, R. L.; Truong, T. N. *J. Chem. Phys.* **1994**, *101*, 10442. (c) Zhang, Q.; Bell, R.; Truong, T. N. *J. Phys. Chem.* **1995**, *99*, 592.

(8) Jensen, J. H.; Gordon, M. S. *J. Am. Chem. Soc.* **1995**, *117*, 8159.

(9) Król-Starzomska, I.; Filarowski, A.; Rospenk, M.; Koll, A.; Melikova, S. *J. Phys. Chem. A* **2004**, *108*, 2131.

(10) (a) Scheiner, S.; Kern, C. W. *J. Am. Chem. Soc.* **1979**, *101*, 4081. (b) Scheiner, S.; Wang, L. *J. Am. Chem. Soc.* **1993**, *115*, 1958. (c) Scheiner, S. *J. Am. Chem. Soc.* **1981**, *103*, 315. (d) Scheiner, S.; Redfern, R.; Szczesniak, M. M. *J. Phys. Chem.* **1985**, *89*, 262. (e) Scheiner, S.; Harding, L. B. *J. Am. Chem. Soc.* **1981**, *103*, 2169.

(11) (a) Bertran, J.; Oliva, A.; Rodríguez-Santiago, L.; Sodupe, M. *J. Am. Chem. Soc.* **1998**, *120*, 8159. (b) Rodríguez-Santiago, L.; Sodupe, M.; Oliva, A.; Bertran, J. *J. Am. Chem. Soc.* **1999**, *121*, 8882.

(12) Pranata, J.; Davis, G. D. *J. Phys. Chem.* **1995**, *99*, 14340.

(13) (a) Nguyen, K. A.; Gordon, M. S.; Truhlar, D. G. *J. Am. Chem. Soc.* **1991**, *113*, 1596. (b) Gordon, M. S. *J. Phys. Chem.* **1996**, *100*, 3974. (c) Chaban, G. M.; Gordon, M. S. *J. Phys. Chem. A* **1999**, *103*, 185. (d) Petrich, J. W.; Gordon, M. S.; Cagle, M. *J. Phys. Chem. A* **1998**, *102*, 1647.

(14) Wu, D. H.; Ho, J. J. *J. Phys. Chem. A* **1998**, *102*, 3582.

(15) Yen, S. J.; Lin, C. Y.; Ho, J. J. *J. Phys. Chem. A* **2000**, *104*, 11771.

(16) Rodriquez, C. F.; Cunje, A.; Shoeib, T.; Chu, I. K.; Hopkinson, A. C.; Siu, K. W. M. *J. Phys. Chem. A* **2000**, *104*, 5023.

(17) (a) Kim, Y. *J. Am. Chem. Soc*. **1996**, *118*, 1522. (b) Lim, J.-H.; Lee, E. K.; Kim, Y. *J. Phys. Chem. A* **1997**, *101*, 2233. (c) Kim, Y.; Hwang, H. J. *J. Am. Chem. Soc.* **1999**, *121*, 4669. (d) Kim, Y. *J. Phys. Chem. A* **1998**, *102*, 3025. (e) Kim, Y.; Lim, S.; Kim, H.-J.; Kim, Y. *J. Phys. Chem. A* **1999**, *103*, 617. (f) Kim, Y.; Lim, S.; Kim, Y. *J. Phys. Chem. A* **1999**, *103*, 6632.

(18) (a) Florián, J.; Hrouda, V.; Hobza, P. *J. Am. Chem. Soc.* **1994**, *116*, 1457. (b) Hrouda, V.; Florián, J.; Polášek, M.; Hobza, P. *J. Phys. Chem.* **1994**, *98*, 4742. (c) Florián, J.; Leszczyński, J. *J. Am. Chem. Soc.* **1996**, *118*, 3010.

(19) Minyaev, R. M. *Chem. Phys. Lett.* **1996**, *262*, 194.

(20) Adamo, C.; Cossi, M.; Barone, V. *J. Comput. Chem.* **1997**, *18*, 1993.

(21) Vishveshwara, S.; Madhusudhan, M. S.; Maizel, J. V., Jr. *Biophys. Chem.* **2001**, *89*, 105.

(22) Lu, D.; Voth, G. A. *J. Am. Chem. Soc.* **1998**, *120*, 4006.

(23) Kryachko, E. S.; Nguyen, M. T. *J. Phys. Chem. A* **2001**, *105*, 153.

(24) Chaudhuri, C.; Jiang, J. C.; Wu, C.-C.; Wang, X.; Chang, H.-C. *J. Phys. Chem. A* **2001**, *105*, 8906.

(25) Taylor, J.; Eliezer, I.; Sevilla, M. D. *J. Phys. Chem. B* **2001**, *105*, 1614.

(26) Tatara, W.; Wójcik, M. J.; Lindgren, J.; Probst, M. *J. Phys. Chem. A* **2003**, *107*, 7827.

(27) Cui, Q.; Karplus, M. *J. Phys. Chem. B* **2003**, *107*, 1071.

(28) Kulhánek, P.; Schlag, E. W.; Koča, J. *J. Am. Chem. Soc.* **2003**, *125*, 13678.

(29) (a) Chou, P.-T.; Yu, W.-S.; Chen, Y.-C.; Wei, C.-Y.; Martinez, S. S. *J. Am. Chem. Soc*. **1998**, *120*, 12927. (b) Chou, P.-T.; Wu, G.-R.; Wei, C.-Y.; Cheng, C.-C.; Chang, C.-P.; Hung, F.-T. *J. Phys. Chem. B* **1999**, *103*, 10042. (c) Chou, P.-T.; Wei, C.-Y.; Wang, C.-R.; Hung, F.-T.; Chang, C.-P. *J. Phys. Chem. A* **1999**, *103*, 1939. (d) Chou, P.-T.; Wu, G.-R.; Wei, C.-Y.; Cheng, C.-C.; Chang, C.-P.; Hung, F.-T. *J. Phys. Chem. B* **2000**, *104*, 7818. (e) Hung, F.-T.; Hu, W.-P.; Li, T.-H.; Cheng, C.-C.; Chou, P.-T. *J. Phys. Chem. A* **2003**, *107*, 3244.

(30) Kryachko, E. S.; Nguyen, M. T.; Zeegers-Huyskens, T. *J. Phys. Chem. A* **2001**, *105*, 1934.

(31) Graf, F.; Meyer, R.; Ha, T.-K.; Ernst, R. R. *J. Chem. Phys.* **1981**, *75*, 2914.

(32) Mitra, S.; Das, R.; Bhattacharyya, S. P.; Mukherjee, S. *J. Phys. Chem. A* **1997**, *101*, 293.

(33) Glaser, R.; Lewis, M. *Org. Lett.* **1999**, *1*, 273.

(34) Brinkmann, N. R.; Tschumper, G. S.; Yan, G.; Schaefer, H. F., III *J. Phys. Chem. A* **2003**, *107*, 10208.

(35) Moreno, M.; Douhal, A.; Lluch, J. M.; Castano, O.; Frutos, L. M. *J. Phys. Chem. A* **2001**, *105*, 3887.

(36) Clementi, E.; Mehl, J.; Niessen, W. V. *J. Chem. Phys.* **1971**, *54*, 508.

(37) Del Bene, J. E.; Kochenour, W. L. *J. Am. Chem. Soc.* **1976**, *98*, 2041.

(38) Schweiger, S.; Rauhut, G. *J. Phys. Chem. A* **2003**, *107*, 9668.

(39) Garcia-Viloca, M.; González-Lafont, A.; Lluch, J. M. *J. Am. Chem. Soc.* **1997**, *119*, 1081.

(40) Hayashi, S.; Umemura, J.; Kato, S.; Morokuma, K. *J. Phys. Chem.* **1984**, *88*, 1330.

(41) Barone, V.; Adamo, C. *J. Phys. Chem.* **1995**, *99*, 15062.

(42) Yamabe, T.; Yamashita, K.; Kaminoyama, M.; Koizumi, M.; Tachibana, A.; Fukui, K. *J. Phys. Chem.* **1984**, *88*, 1459.

(43) Guallar, V.; Douhal, A.; Moreno, M.; Lluch, J. M. *J. Phys. Chem. A* **1999**, *103*, 6251.

(44) Makowski, M.; Liwo, A.; Wrobel, R.; Chmurzynski, L. *J. Phys. Chem. A* **1999**, *103*, 11104.

(45) Norikane, Y.; Nakayama, N.; Tamaoki, N.; Arai, T.; Nagashima, U. *J. Phys. Chem. A* **2003**, *107*, 8659.

(46) (a) Ahn, D.-S.; Park, S.-W.; Jeon, I.-S.; Lee, M.-K.; Kim, N.-H.; Han, Y.-H.; Lee, S. *J. Phys. Chem. B* **2003**, *107*, 14109. (b) Park, S.-W.; Ahn, D.-S.; Lee, S. *Chem. Phys. Lett.* **2003**, *371*, 74.

(47) Shimoni, L.; Glusker, J. P.; Bock, C. W. *J. Phys. Chem.* **1996**, *100*, 2957.

(48) (a) Pan, Y.; McAllister, M. A. *J. Am. Chem. Soc.* **1997**, *119*, 7561. (b) Pan, Y.; McAllister, M. A. *J. Org. Chem.* **1997**, *62*, 8171. (c) Smallwood, C. J.; McAllister, M. A. *J. Am. Chem. Soc.* **1997**, *119*, 11277. (d) Pan, Y.; McAllister, M. A. *J. Am. Chem. Soc*. **1998**, *120*, 166. (e) Kumar, G. A.; McAllister, M. A. *J. Am. Chem. Soc.* **1998**, *120*, 3159.

(49) (a) Li, P.; Bu, Y. *J. Phys. Chem. A* (submitted for publication). (b) Li, P.; Bu, Y. *J. Chem. Phys.* (in press).

(50) Periquet, V.; Moreau, A.; Carles, S.; Schermann, J. P.; Desfrançois, C. *J. Electon Spectrosc. Relat. Phenom.* **2000**, *106*, 141.

(51) Chen, E. S. D.; Chen, E. C. M.; Sane, N.; Shulze, S. *Bioelectrochem. Bioenerg.* **1999**, *48*, 69.

(52) Oie, T.; Loew, G. H.; Burt, S. K.; MacElroy, R. D. *J. Am. Chem. Soc.* **1984**, *106*, 8007.

(53) Jensen, J. H.; Baldridge, K. K.; Gordon, M. S. *J. Phys. Chem.* **1992**, *96*, 8340.

(54) (a) Remko, M.; Rode, B. M. *Chem. Phys. Lett.* **2000**, *316*, 489. (b) Remko, M.; Rode, B. M. *Phys. Chem. Chem. Phys.* **2001**, *3*, 4667.

(55) Kinser, R. D.; Ridge, D. P.; Hvistendahl, G.; Rasmussen, B.; Uggerud, E. *Chem.—Eur. J.* **1996**, *2*, 1143.

(56) Grewal, R. N.; Aribi, H. E.; Smith, J. C.; Rodriquez, C. F.; Hopkinson, A. C.; Siu, K. W. M. *Int. J. Mass Spectrom.* **2002**, *219*, 89.

(57) (a) Li, P.; Bu, Y.; Ai, H. *J. Phys. Chem. A* **2003**, *107*, 6419. (b) Li, P.; Bu, Y.; Ai, H. *J. Phys. Chem. B* **2004**, *108*, 1405. (c) Li, P.; Bu, Y.; Ai, H.; Cao, Z. *J. Phys. Chem. A* **2004**, *108*, 4069. (d) Li, P.; Bu, Y.; Ai, H. *J. Phys. Chem. A* **2004**, *108*, 1200. (e) Li, P.; Bu, Y. *J. Phys. Chem. A* (submitted for publication).

(58) (a) Gonzalez, C.; Schlegel, H. B. *J. Chem. Phys.* **1989**, *90*, 2154. (b) Gonzalez, C.; Schlegel, H. B. *J. Phys. Chem.* **1990**, *94*, 5523.

(59) Jensen, J. H.; Gordon, M. S. *J. Am. Chem. Soc.* **1991**, *113*, 7917.

(60) Steinfiled, J. I.; Francisco, J. S.; Hase, W. L. *Chemical Kinetic and Dynamics*; Prentice Hall: Englewood Cliffs, NJ, 1989.

(61) Wigner, E. *Z. Phys. Chem. B* **1932**, *19*, 203.

(62) (a) Barone, V.; Cossi, M.; Tomasi, J. *J. Comput. Chem.* **1998**, *19*, 404. (b) Barone, V.; Cossi, M. *J. Phys. Chem. A* **1998**, *102*, 1995.

(63) Foresman, J. B.; Keith, T. A.; Wiberg, K. B.; Snoonian, J.; Frisch, M. J. *J. Phys. Chem.* **1996**, *100*, 16098.

(64) (a) Li, X.; Sevilla, M. D.; Sanche, L. *J. Am. Chem. Soc.* **2003**, *125*, 8916. (b) Li, X.; Sanche, L.; Sevilla, M. D. *J. Phys. Chem. A* **2002**, *106*, 11248.

(65) Lee, I.; Kim, C. K.; Han, I. S.; Lee, H. W.; Kim, W. K.; Kim, Y. B. *J. Phys. Chem. B* **1999**, *103*, 7302.

(66) Kovacevic, B.; Maksic, Z. B. *Org. Lett.* **2001**, *3*, 1523.

(67) Boys, S. F.; Bernardi, F. *Mol. Phys.* **1970**, *19*, 553.

(68) Frisch, M. J.; Trucks, G. W.; Schlegel, H. B.; Scuseria, G. E.; Robb, M. A.; Cheeseman, J. R.; Zakrzewski, V. G.; Montgomery, J. A., Jr.; Stratmann, R. E.; Burant, J. C.; Dapprich, S.; Millam, J. M.; Daniels, A. D.; Kudin, K. N.; Strain, M. C.; Farkas, O.; Tomasi, J.; Barone, V.; Cossi, M.; Cammi, R.; Mennucci, B.; Pomelli, C.; Adamo, C.; Clifford, S.; Ochterski, J.; Petersson, G. A.; Ayala, P. Y.; Cui, Q.; Morokuma, K.; Malick, D. K.; Rabuck, A. D.; Raghavachari, K.; Foresman, J. B.; Cioslowski, J.; Ortiz, J. V.; Stefanov, B. B.; Liu, G.; Liashenko, A.; Piskorz, P.; Komaromi, I.; Gomperts, R.; Martin, R. L.; Fox, D. J.; Keith, T.; Al-Laham, M. A.; Peng, C. Y.; Nanayakkara, A.; Gonzalez, C.; Challacombe, M.; Gill, P. M. W.; Johnson, B.; Chen, W.; Wong, M. W.; Andres, J. L.; Gonzalez, C.; Head-Gordon, M.; Replogle, E. S.; Pople, J. A. *Gaussian 98*, revision A.9; Gaussian Inc.: Pittsburgh, PA, 1998.

(69) Benderskii, V. A.; Makarov, D. E.; Wight, C. A. *Adv. Chem. Phys.* **1994**, *88*, 1.

(70) Rauhut, G. *Phys. Chem. Chem. Phys* **2003**, *5*, 791.

(71) Colson, A. D.; Besler, B.; Close, D. M.; Sevilla, M. D. *J. Phys. Chem.* **1992**, *96*, 661.